CFD Evaluation of OECD PSBT Geometry Effects Based on Fluid Temperature Measurements

Y. Xu, Y. Sung and E. Tatli
Westinghouse Electric Company, 1000 Westinghouse Drive, Cranberry Township, PA 16066, USA
xuy@westinghouse.com; sungy@westinghouse.com; tatlie@westinghouse.com

ABSTRACT

Turbulent mixing, void and Departure from Nucleate Boiling (DNB) experimental data from the Organization for Economic Co-operation and Development / Nuclear Regulatory Commission (OECD/NRC) Pressurized Water Reactor (PWR) Sub-channel and Bundle Tests (PSBT) international benchmark exercises are available for benchmarking system, sub-channel and Computational Fluid Dynamics (CFD) codes simulating fuel thermal-hydraulic behavior. In order to better understand the mixing test data and the uncertainties in the rod bundle and spacer grid geometric parameters, several CFD models with different configurations and numbers of spacer grids were built in STAR-CCM+ (CD-adapco) based on previous benchmarking experience for similar geometries to the PSBT rod bundle test section. Geometry effects on fluid temperature distribution at sub-channel exits were explored by comparing the CFD predicted results to the measured test data in the PSBT Phase II/Exercise 1. The CFD evaluation results show that spacer grids with mixing vanes in the test bundle were most likely installed with alternating 90º rotations, consistent with the actual fuel design practices at the time. The results from the CFD simulations incorporating the spacer grid rotation are in better agreement with the measured test data. The CFD evaluation also indicates that fully developed thermal mixing is associated with the number of spacer grids in the test bundle. CFD modeling and simulation of the full length test bundle and radial geometry is recommended for future benchmark exercises.

KEYWORDS
CFD, PSBT Rod Bundle, Mixing Vanes, Orientation of Spacer Grids, Turbulent Mixing

1. INTRODUCTION

PWR Sub-Channel and Bundle Tests (PSBT) are a series of thermal hydraulic tests conducted by NUPEC in typical PWR fuel bundles and operated under prototypical PWR conditions with a wide range of operating conditions of system pressures, heating powers, inlet fluid temperatures and flow rates. The benchmark database [1] composed by the Pennsylvania State University sponsored by OECD and NRC includes high quality and high resolution experimental data of void fraction distribution, sub-channel fluid temperatures and DNB powers of single and two-phase flows in single sub-channel and rod bundle

geometries under steady state and transient conditions. PSBT database has been used for many code benchmarks and assessments in pressure drop, void fraction distribution and steady state or transient DNB powers as summarized in [2].

Phase II/Exercise 1, which is the focus herein, includes fluid temperature measurement test data (thermal mixing). In thermal mixing tests, in the test section named as PSBT A1 [1], the fluid temperatures at the center of sub-channels downstream of the end of heated length were measured with thermocouples under steady state conditions. PSBT A1 section consisted of a 5x5 rod bundle with 25 heated rods, three types of spacer grids and Type C radial power distribution. Type C radial power distribution, an aggressive distribution (four times between hot and cold rods) compared to others [5], was applied to the rod bundle, creating strong thermal gradients across the cross section which may serve well as a candidate for code assessments and benchmarking, such as thermal diffusion coefficients benchmarking conducted in [3, 4].

Since the test series was primarily designed for assessments and benchmarking of system and/or sub-channel codes, detailed geometry information was neither disclosed nor available, particularly the information on the spacer grids. The spacer grid design information was obtained from one of the benchmark participants as stated in [2]. Insufficient information is a big challenge for conducting accurate CFD analyses. On the other hand, CFD codes are capable of capturing geometric effects when computational mesh and numerical algorithms are appropriately selected. This test data may provide an opportunity for using CFD codes to determine further geometry details, such as mixing vane orientations in actual operated tests.

Due to the periodic and/or repeatable features in rod bundle designs, computational models with partial lengths are generally used in CFD benchmarking practices [5, 6, 7, and 8] without loss in accuracy in order to reduce computing costs. This may be appropriate for cases in which the independence of the flow field to number of spacer grids is demonstrated, but it may not be the case for thermal mixing cases since heating power is added continuously along the length of the test section.

Several CFD models with different lengths and spacer grid orientations were created to investigate the geometric effects on thermal mixing in rod bundles. A possible grid orientation was identified and an appropriate CFD modeling approach for thermal mixing simulations in PWR rod bundles was recommended.

2. PSBT Thermal Mixing Tests and the Development of the CFD Modeling Approach

2.1. PSBT Fluid Temperature Tests and Data

Among PSBT series, Phase II/ Exercise 1 was devoted to fluid temperature measurements (thermal mixing). The test section used in this exercise is schematically shown in Figure 1 - a 5x5 rod bundle without any unheated thimble tubes. It consisted of two (2) spacer grids with no mixing vanes (NMV) at the beginning and at the end of the heated length (BOHL and EOHL). Between these two NMV grids, seven (7) spacer grids with mixing vanes (MVG) and eight (8) simple support grids (SSG) were distributed alternatively along the heated section. The axial locations of the grids (defined at their bottom edges) are tabulated in Figure 2. The table also includes the locations of fluid temperature measurements (FTM) and the test section configuration with rotated MVGs (referred to as MVR). The 3D images of these grids are copied from [1] as shown in Figure 1. An axially uniform power profile was applied between BOHL and EOHL in Type C distribution in the radial direction (shown in Figure 2). Coolant temperatures were measured by thermocouples placed at the centers of sub-channels located 457 mm from the EOHL. Sixty tests were conducted with various mass fluxes, system pressures, coolant inlet temperatures, and heating powers. Several tests were marked and recommended by the database composer for assessments, and data set 01-5343 was selected for the CFD simulation. Since the CFD

models use different lengths, it is difficult (if not impossible) to have appropriate inlet temperatures so that fluid temperatures at the FTM are the same for different CFD simulations. Furthermore, it is the temperature gradients, not the absolute temperature values that indicate thermal mixing behavior. Of course, the latter plays a secondary role in estimating fluid properties. Therefore, it is more convenient to use temperature differences relative to cross section averaged values for comparison among different CFD simulations. The operating conditions and the temperature difference data of this test are listed in Figure 2.

2.2. Development of the CFD Modeling Approach

It was assumed that the far away upstream geometry features had little effect on flow and heat transfer downstream in rod bundles, such as PWR fuel assemblies [5]. Generally, CFD models are built for partial length in order to save computing time. However, it is not clear how many spacer grids are sufficient in order to be able to validate this assumption for this particular case, or whether or not fluid flow and thermal mixing behave the same.

In this exercise, partial length and full length (including all grids) CFD models were developed. The best practices learned from previous benchmarking exercises [9] were adopted in the selection of mesh generation settings, turbulence models, and numerical algorithms.

Since there was no information on MVG orientation and their relationship to radial power distribution in the test specifications [1], many combinations of MVG orientations, and the power distribution and MVG orientations were possible. In reality, the most possible variation is that some of MVGs may be rotated from others, consistent with the grid rotations in actual fuel assemblies: i.e., 3 MVGs or 4 MVGs rotated. The 4 MVGs rotation can be realized using radial power rotation. Therefore, radial power rotation can be used to evaluate its relationship with the MVG orientation without building a new geometry.

In order to address the above issues, a total of six CFD models were built in STAR-CCM+ [10]. Their details are listed in Table I, including domain lengths, number of grids and their orientations. The last column in the table shows number of computational cells in each model. The number in the parenthesis was obtained from a smaller base size for mesh independence check. All models have the same outlet location, about L/D=35 from the FTM. At the inlets, constant mass flow rate and uniform temperature profiles were applied. All solid surfaces, including the side casing, were treated as no-slip wall boundaries. Typical meshes at the outlet and on MVG region are shown in Figure 3. Very fine computational meshes were built to capture the small geometric features of MVGs, which could have significant effects on the mixing performance. The prism layers were created near solid surfaces and corners with reasonably good quality. The mesh was extended axially in order to save mesh cells since the flow velocity is dominantly large in the axial direction.

Fluid temperatures were extracted for each sub-channel as numbered in Figure 2. These points are defined at the center for whole sub-channels while minor adjustments are needed for side and corner sub-channels. The plane of these points is located at the FTM (4115 mm from the BOHL). A straight line along x-axis (red dotted line in Figure 2) is defined on this plane for line plots of velocity and temperature. Similarly, another parallel line is created on the plane of 2856 mm where mixing effects involving different number of MVGs are demonstrated.

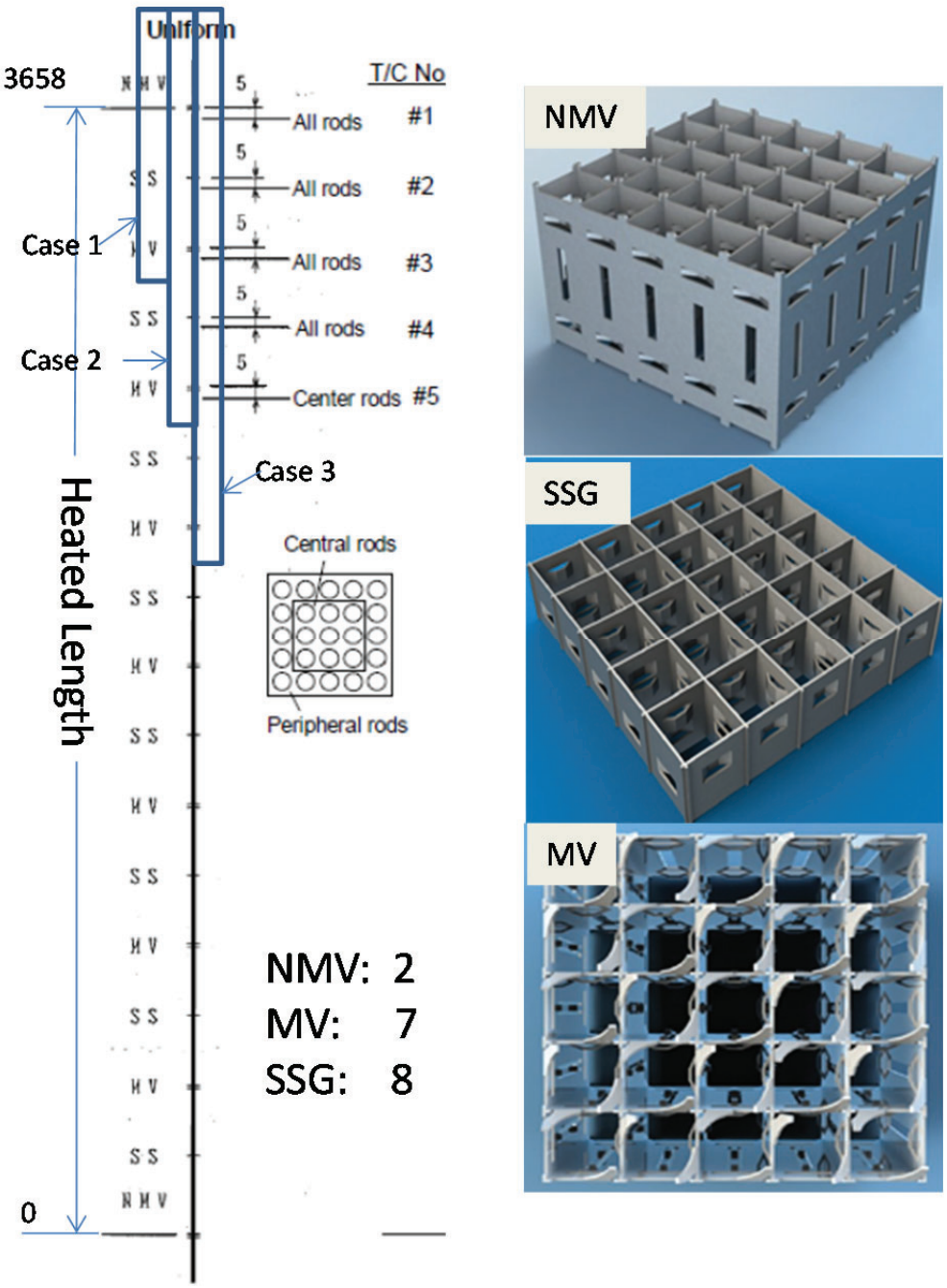

Figure 1 Test Section and Spacer Grids [1]

Power Factors and Sub-Channel IDs

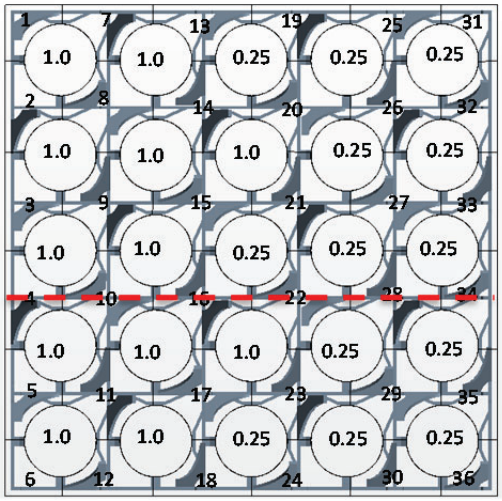

Temperature Differences at FTM (°C)

14.12	12.72	4.72	2.52	-3.68	-8.08
16.32	14.72	6.02	1.42	-5.08	-8.68
12.42	10.02	5.82	-3.68	-7.78	-10.28
9.92	5.52	-0.78	-8.58	-9.38	-11.58
9.42	7.02	-0.48	-10.78	-12.88	-14.68
9.52	7.62	4.12	-6.98	-13.48	-17.18

Elevations of Components

PSBT (mm)	A1	A1MVR
4500	Outlet	
4115	FTM	
3658	EOHL	
3658	NMV (EOHL)	
3429	SS	
3200	MV	MV
2972	SS	
2743	MV	MVR
2515	SS	
2286	MV	MV
2057	SS	
1829	MV	MVR
1600	SS	
1372	MV	MV
1143	SS	
914	MV	MVR
686	SS	
457	MV	MV
229	SS	
0	NMV (BOHL)	
-25	Inlet	

Test Conditions

System Pressure (MPa)	14.71
Mass Flow Rate (kg/s)	3.4273
Heat Flux (W/m^2)	750797.8
Inlet Temperature (°C)	165.3

Figure 2 Test Conditions, Power Distribution, Test Data, and Component Configurations

Table I. Details of the CFD Domains

CFD Domain	Length (mm)	SSG	NMV	MVG	MVR	# of Cells (*10^6)
MV-C1	3086 to 4500	1	1	1	0	6.35 (13.71*)
MV-C2	2629 to 4500	2	1	2	0	12.92
MV-A1	-25 to 4500	8	2	7	0	40.25
MVR-C2	2629 to 4500	2	1	1	1	9.86
MVR-C3	2172 to 4500	3	1	2	1	13.17
MVR-A1	-25 to 4500	8	2	4	3	30.11

(*mesh generation base size equal to 0.6 mm vs. 0.8 mm in original mesh)

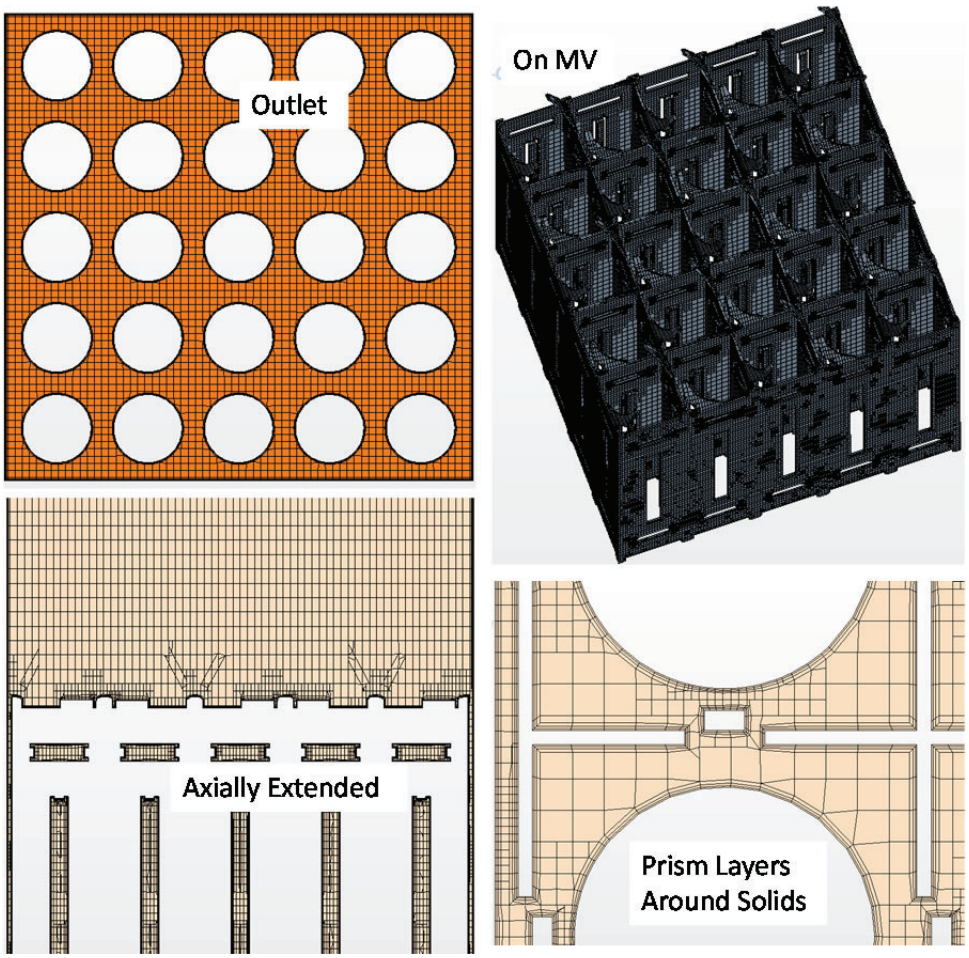

Figure 3 Typical mesh scenes

3. Evaluation of CFD Simulation Results

CFD models of the PSBT test section A1 [1] were built and run using STAR-CCM+ v8.06. Steady state RANS modeling was adopted with standard k-ε turbulence model and two-layer all y+ wall treatments. A default quadratic relationship between strain and stress was chosen. Fluid density, dynamic viscosity and thermal conductivity were tabulated versus temperature while specific heat was fitted with a 4^{th} order polynomial as a function of temperature. The results were judged converged when monitored variables (local axial velocity, turbulent kinetic energy and temperature) and the residuals stabilized reaching constant values, special attention paid to the energy balance in the domain. The simulation results were extracted from the last iteration. Although temperature gradients exist across each sub-channel, it was verified that variations between averaging across each sub-channel and the values at center points are. Therefore, only the values at the center points were used in following evaluations.

3.1. CFD Simulation without MVG Rotation

The first set of CFD models was built based on the information disclosed in [1]. Since there is no specification regarding MVG orientations and the symbols of the MVGs in Figure 1 are identical for all MVGs, it was assumed that the MVGs were aligned identically in the test section. Three different CFD domain lengths were used to investigate the upstream condition effects on thermal mixing. A typical temperature contour plot (MV-C2) is shown in Figure 4a. A high temperature region and a low

temperature region appear at the upper left and lower right corners, respectively, due to swirling flows produced by the MVGs. Thermal mixing is clearly seen from the hot region to the cold region through the temperature gradients. The fluid temperatures at the FTM from all three MV models are compared with the test data in Figure 4b. Overlapping the two results from MV-C1 shows that mesh independence is achieved with the selected mesh settings. The full length model significantly over-predicts temperature differences between the hot and the cold regions, indicating under-prediction of thermal mixing. This indicates that there may be some feature missing in the model. MV-C2 produced the best match with the data, further proving that inappropriate boundary conditions and geometry features could produce misleading information.

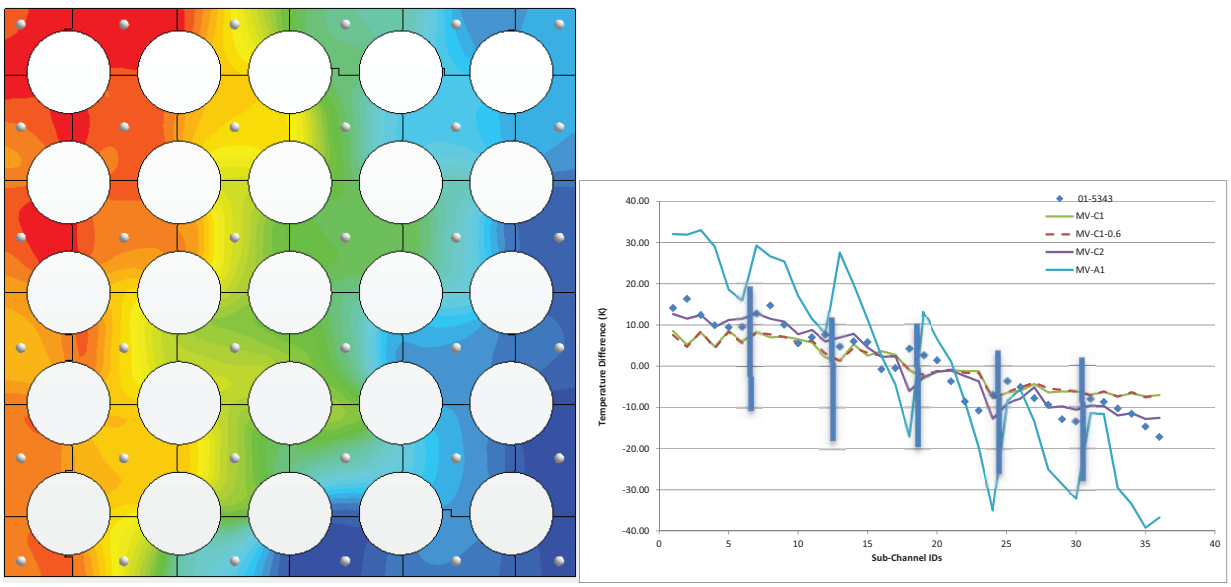

a Temperatures at FTM b MV results vs. test data

Figure 4 Temperatures at FTM of MV Cases

3.2. CFD Simulation with MVG Rotation

The results in Section 3.1 suggested possible incorrect geometry features existed in the models. One of the most likely situations was the orientations of the MVGs. It is common practice that MVGs are rotated alternatively, i.e. the downstream MVG is rotated by 90^o of the upstream one, and the next one is rotated by -90^o, and so on. The second set of the CFD models was built based on this assumption (MVR-C2, MVR-C3, and MVR-A1) with other parameters identical to the first set. Similar to the MVG without rotation cases, a hot region and a cold region still co-exist in the MVR cases as seen in Figure 5a. However, the hot spots appear at quite different locations, indicating better mixing from the MVR designs. Furthermore, comparison of temperatures at the FTM between the CFD and the test data show the significant improvements in CFD predictions. Especially, predictive errors are almost reduced to half in the full length model. This indicates that the misalignment of the MVGs was one of the major error sources in the first set of CFD models. In other words, CFD tools are capable of finding possible simulation errors when appropriate modeling approaches are pre-determined. This also shows that appropriately assessed CFD tools can be utilized to perform design optimization for appropriate physical processes.

A closer look may reveal mismatches from the CFD simulations. Temperature trends of the same columns (indicated by the vertical solid lines in Figures 4b and 5b) are inconsistent or opposite between the test and the simulations, gradually decreasing from a lower number sub-channel to a higher one, particularly

in Columns 5 and 6 (i.e. cold region) in the test. Sub-Channel 24 has a lower temperature for both MV and MVR models, while it was higher than the neighboring sub-channels in the test data. Larger error from the full length model indicates that turbulent dissipation may be over-predicted in these models.

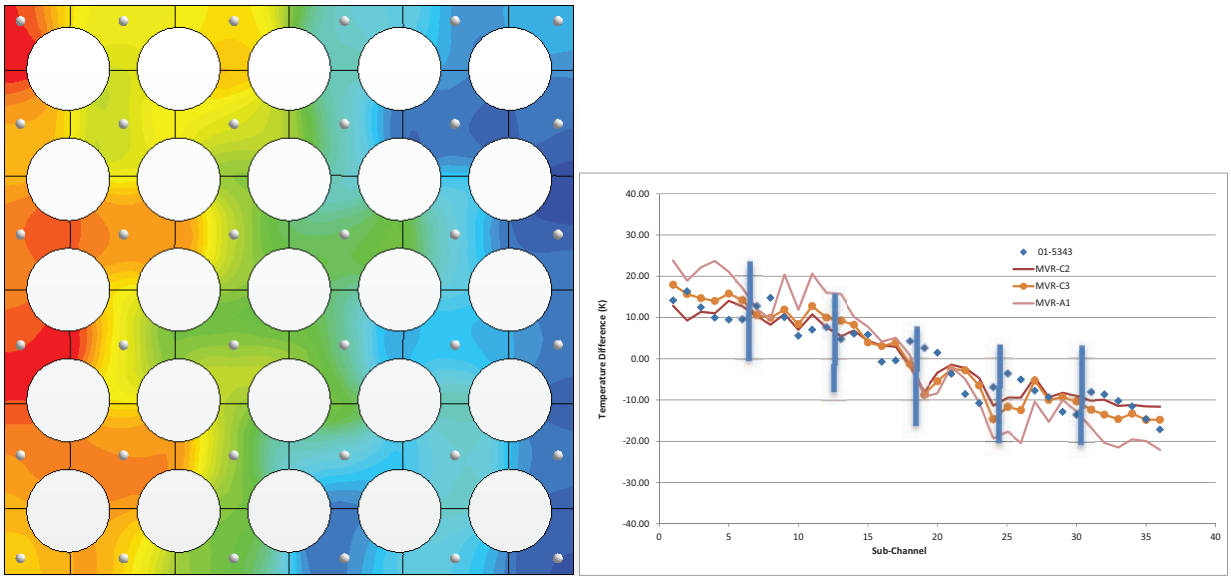

a Temperatures at FTM b MVR results vs. test data

Figure 5 Temperatures at FTM of MVR Cases

The prediction performance of the above models for thermal mixing may be better viewed graphically. A channel error ($channel\ error = \frac{\sum_{k=1}^{36}|T_{data}-T_{CFD}|}{36}$) is defined for an average error between the test data and the CFD results over all of the sub-channels. Figure 6 shows a plot of the channel errors of the aforementioned models.

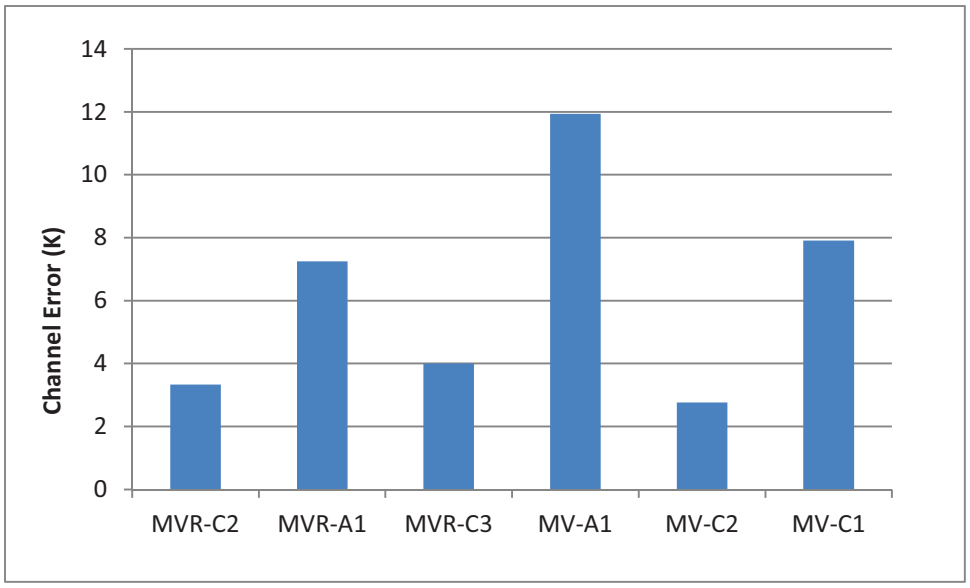

Figure 6 Channel Errors (Performance Indicator) of CFD Models

3.3. Flow Fields due to Inlet Boundary Conditions

Lateral velocity is a key indicator of thermal mixing within sub-channels. Vector plots of lateral velocities at the FTM of the MV models are depicted in Figures 7a, 7b, and 7c. The velocity scale is from 0 to 0.02 m/s for all of the plots. It can be seen that the velocity distribution is quite similar for all three cases, but their magnitudes become smaller as the CFD domain becomes longer. This also indicates an over-prediction of turbulent dissipation. Axial velocity was extracted from a line at the FTM plane as shown in Figure 7a. The results are presented in Figure 7d. Axial velocity is larger in the hot region due to lower density. The differences of axial velocities between hot and cold regions appear closely correlated with temperature gradients (or thermal mixing); MV-A1 has the largest differences with most under-prediction of thermal mixing; MV-C1 has the smallest with over-prediction of thermal mixing.

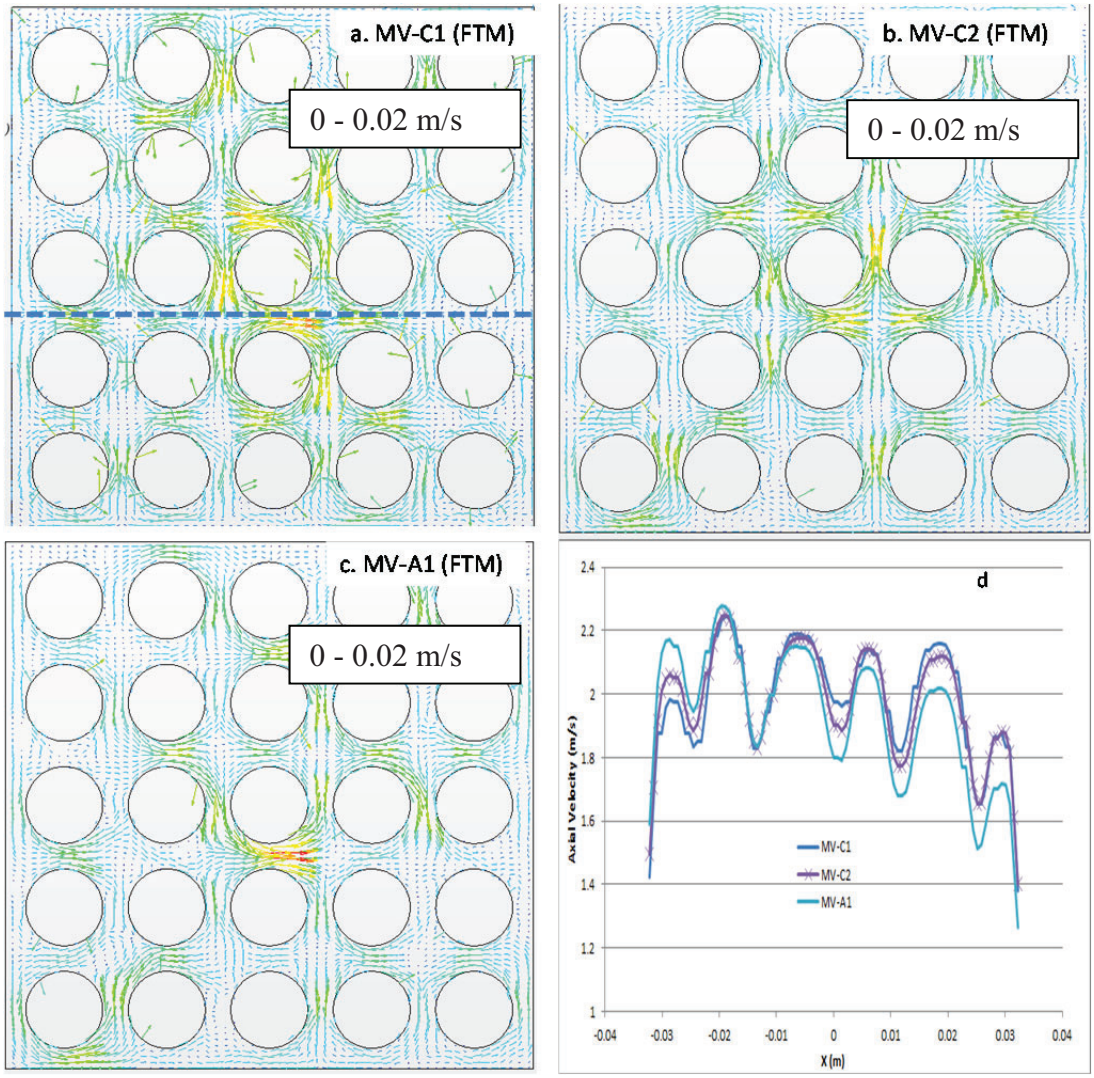

Figure 7 Flow Fields at FTM of MV Models

As a comparison of MV models, the flow fields of MVR models are plotted in Figure 8. The MV at the highest elevation is shown in Figure 2 for illustrating the relationship between lateral

velocity direction and the MV orientation. A swirling flow pattern around rods was created by the vanes. It can also be observed that high lateral flow appears in the channels away from the bundle center, indicating better mixing flow in the MVR models than in the MV models. The differences of the axial velocity magnitudes (seen in Figures 7d and 8d) are mainly due to the different inlet temperatures used.

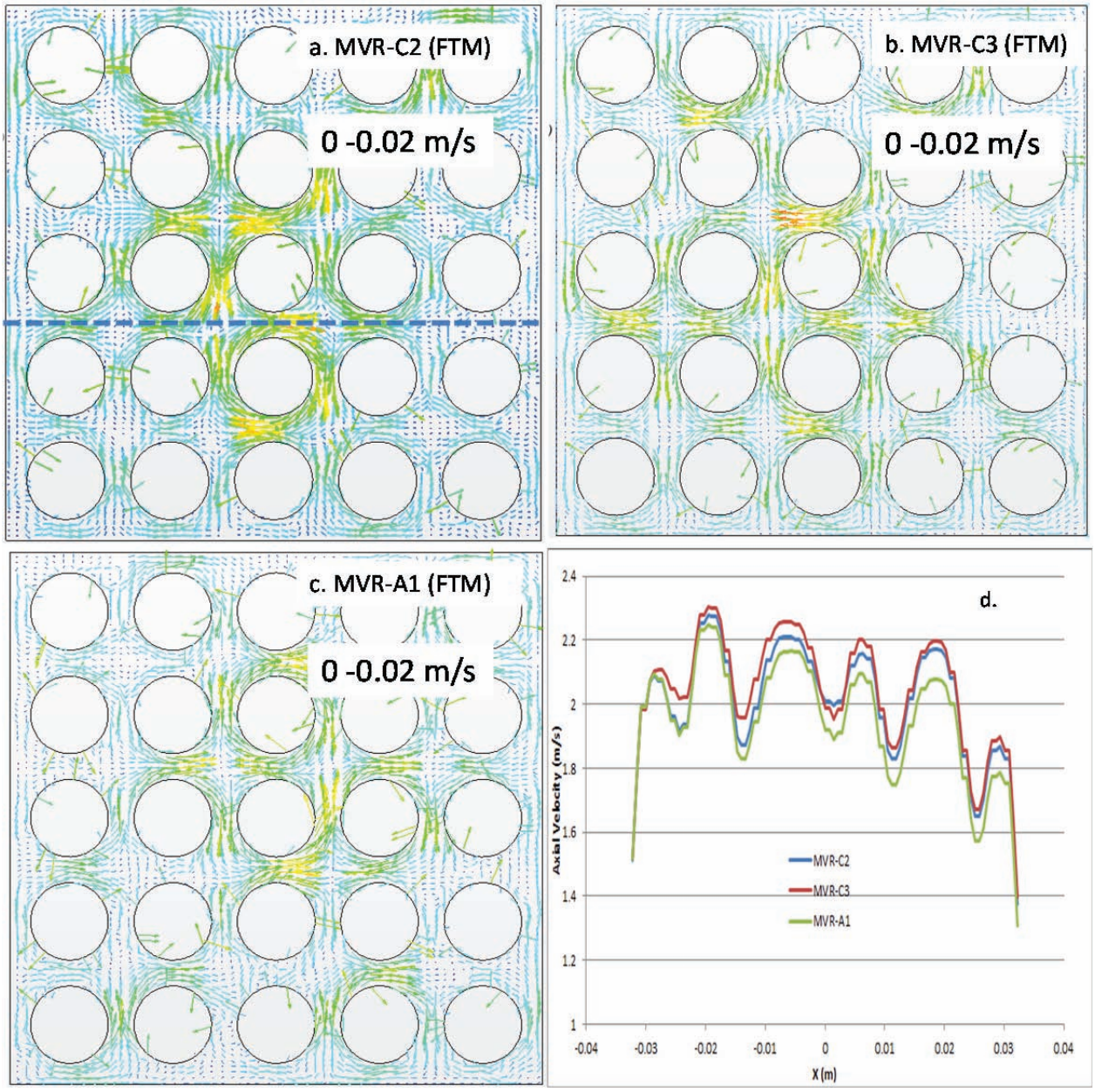

Figure 8 Flow Fields at FTM of MVR Models

It was pointed out that many researchers used one or two spans of rod bundles for the PSBT benchmarking exercises [5, 6, 7 and 8]. This may be appropriate for hydraulic variables such as velocity and turbulent quantities. It is questionable for predicting the fluid temperature

distribution since heating power is added in the axial direction continuously. Figure 9 shows the velocity components and fluid temperatures along the dotted line shown in Figure 8 at Elevation 2856 mm. This location has one MVG for MVR-C2, two MVGs for MVR-C3 and six MVGs for MVR-A1 from the inlet, where uniform temperature and constant mass flow were applied. It can be seen that the velocity profiles are virtually independent of the number of MVGs at upstream, particularly the lateral velocity components. Visible differences in axial velocity profiles are mainly from the density differences caused by local fluid temperatures. On the other hand, the distributions of temperature differences (calculated based on its average across the cross section of the elevation) are quite different. The more MVGs are involved, the larger temperature differences. This clearly indicates that a single MVG cannot achieve complete thermal mixing.

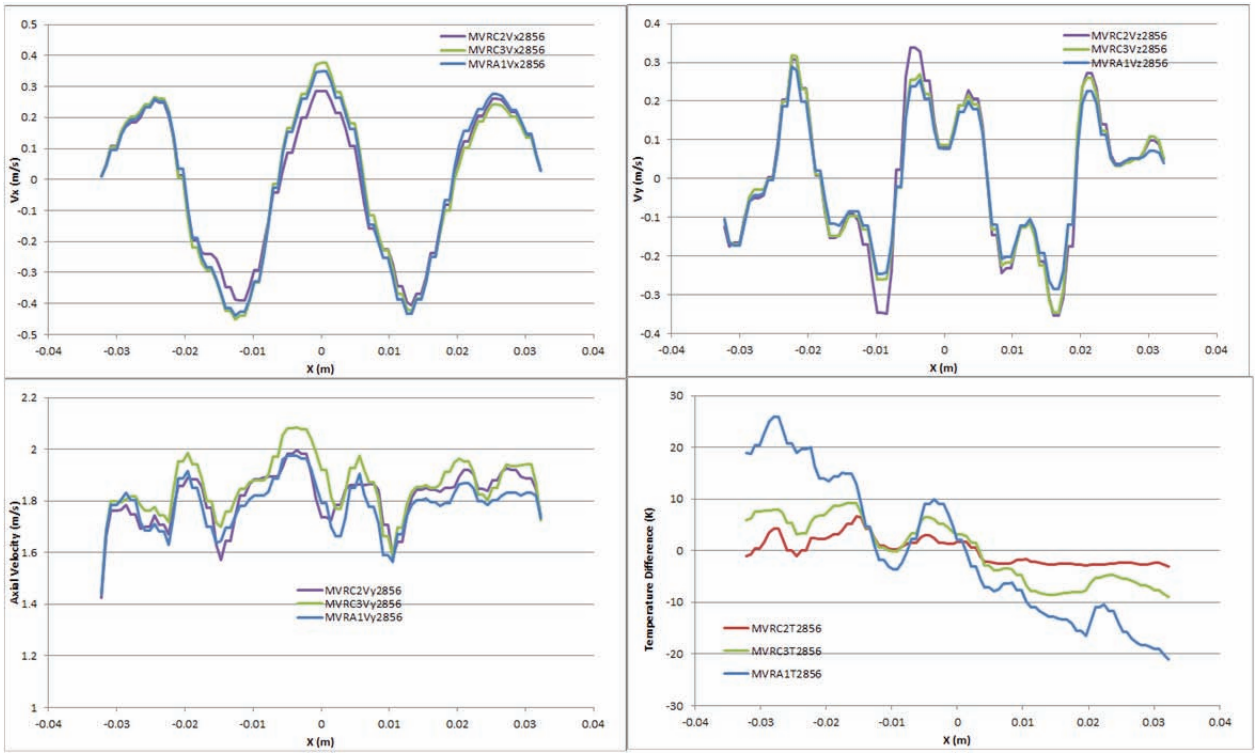

Figure 9 Velocity and Temperature Fields at 2856 mm of MVR Models

4. CONCLUSIONS

The PSBT fluid temperature measurement test data (A1) was used for CFD modeling and simulations using STAR-CCM+ with different mixing vane orientations and domain lengths. The CFD model was able to identify missing geometry features with adoption of the best practice guidelines and lessons learned from similar prior benchmark practices. It can be concluded that the mixing vane spacer grids in the rod bundle tests were rotated, consistent with the actual fuel assembly design at the time. Different from flow fields, which were not sensitive to number of upstream mixing vanes involved, thermal mixing (temperature gradients) demonstrated much longer upstream effects. A CFD model for the whole heated length is recommended for thermal mixing benchmark or assessment; otherwise, additional justification is needed on defining the inlet boundary conditions, particularly the inlet temperature distribution.

NOMENCLATURE

BOHL	Beginning Of Heated Length
CFD	Computational Fluid Dynamics
DNB	Departure from Nucleate Boiling
EOHL	End Of Heated Length
FTM	Fluid Temperature Measurement
MV	Mixing Vane Model
MVG	Mixing Vane Grid
MVR	Rotated Mixing Vane Model
NMV	Non-Mixing Vane
NRC	Nuclear Regulatory Commission
NUPEC	NUclear Power Engineering Corporation
OECD	Organization for Economic Co-operation and Development
PSBT	PWR Sub-Channel and Bundle Test
SSG	Simple Support Grid

REFERENCES

1. A. Rubin, M. Avramova, and H. Utsuno, "OECD/NRC benchmark based on NUPEC PWR subchannel and bundle tests (PSBT) volume I: experimental database and final problem specifications," Tech. Rep. NEA/NSC/DOC(2010)1, USA, NRC/OECD Nuclear Energy Agency.
2. M. Avramova, A. Rubin, and H. Utsuno, "Overview and Discussion of the OECD/NRC Benchmark Based on NUPEC PWR Subchannel and Bundle Tests", Science and Technology of Nuclear Installations Volume 2013, Article ID 946173, 20 pages, http://dx.doi.org/10.1155/2013/946173
3. Y. Sung, R. L. Oelrich Jr., C. C. Lee, N. Ruiz-Esquide, M. Gambetta, C. M. Mazufri, "Benchmark of Subchannel Code VIPRE-W with PSBT Void and Temperature Test Data", Science and Technology of Nuclear Installations, Volume 2012, Article ID 757498, 11 pages doi:10.1155/2012/757498
4. M. Valette, "Subchannel and Rod Bundle PSBT Simulation With CATHARE-3", The 14th International Topical Meeting on Nuclear Reactor Thermalhydraulics, NURETH-14-132, Toronto, Ontario, Canada, September 25-30, 2011
5. K. Ikeda, M. Hoshi, "Development of Mitsubishi High Thermal Performance Grid (CFD Applicability for Thermal Hydraulic Design," JSME International Journal Series B, Vol. 45, No.3, 2002.
6. M. E. Conner, E. Baglietto, A. M. Elmahdi, "CFD Methodology and Validation for Single-phase flow in PWR fuel assemblies", Nuclear Engineering and Design, 240, pp. 2088-2095, 2010
7. C. Pena-Monferrer, J. L. Munoz-Cobo, S. Chiva, "CFD Turbulence Study of PWR Spacer-Grids in a Rod Bundle", Science and Technology of Nuclear Installations, Volume 2014, Article ID 635651, 15 pages, http://dx.doi.org/10.1155/2014/635651
8. C. P. Tzanos, "Computational Fluid Dynamics for the analysis of light water reactor flows", Nuclear Technology, Volume 147, No. 2, August 2004, pages: 181-190
9. M. E. Conner, Z. E. Karoutas, Y. Xu, "Westinghouse CFD Modeling and Results for EPRI NESTOR CFD Round Robin Exercises of PWR Rod Bundle Testing", NURETH-16 Paper-13601.
10. STAR-CCM+8.06, www.cd-adapco.com